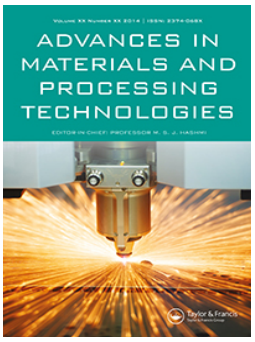

Advances in Materials and Processing Technologies

ISSN: (Print) (Online) Journal homepage: https://www.tandfonline.com/loi/tmpt20

Analysis and construction of a pneumatic-powered portable friction stir welding tool for polymer joining

Raheem Al-Sabur, M. Serier & A. N. Siddiquee

ADVANCES IN MATERIALS AND PROCESSING TECHNOLOGIES
https://doi.org/10.1080/2374068X.2023.2173769

Analysis and construction of a pneumatic-powered portable friction stir welding tool for polymer joining

Raheem Al-Sabur [a], M. Serier [b] and A. N. Siddiquee [c]

[a]Mechanical Department, Engineering College, University of Basrah, Basrah, Iraq; [b]Mechanical Engineering, Institute of Technology, University of Relizane, Relizane, Algeria; [c]Department of Mechanical Engineering, Jamia Millia Islamia, New Delhi, India

ABSTRACT

The increasing use of polymer products in transportation and almost all sectors is a distinctive sign of the current decade. On-site repair of defects along the spatial path are important advantages of a portable welding and repair system. The current article presented an in-house developed pneumatically powered portable set-up and tool for defect repair based on friction stir welding (FSW). The suggested tool can be used for welding polymer products such as car bumpers, motorboats, and polymer vessels. Further, acrylonitrile butadiene styrene (ABS) polymer specimens were joined by FSW and friction stir spot welding (FSSW), and the maximum temperature was monitored. FSW process parameters: rotational speed and traversing velocity, and FSSW parameter: rotational speed and dwell time, were varied, and the design of experiment-based investigations was carried out. Response surface method (RSM) and analysis of variance (ANOVA) were used to analyse the results. The acceptable results were obtained for rotational speed of less than or equal to 1100 rpm and welding velocity lower than 6.5 mm/min (for FSW). Good quality welds were obtained for dwell time equal to or higher than 25 s (for FSSW). The preferred temperature for a good quality weld was found to be 105°C in both processes.

ARTICLE HISTORY
Accepted 23 January 2023

KEYWORDS
FSW; pneumatic; polymer; ABS; acrylonitrile butadiene styrene

1. Introduction

The Sustainable Development Goals (SDGs) for energy savings have created a massive push for weight loss [1]. The weight savings without affecting the design and operational safety of welded parts is one of the day's biggest challenges. The pursuit of weight reduction has made way for the increasing use of polymers.

Polymer-based materials rapidly replace metals in many applications for many reasons [2]. In the plastics industry, as it is now, new business models and innovations are significant, and they must go hand in hand with constant adaptation to the current environment. Developing new business models does not always necessitate new technology; reorganising business models and adopting new ideas from other industries can result in innovations [3]. The fast-growing potential of good use of polymeric materials

CONTACT Raheem Al-Sabur raheem.musawel@uobasrah.edu.iq Mechanical Department, Engineering College, University of Basrah, Basrah, Iraq

cannot be harnessed fully unless better-joining methods of these materials are perfected. Traditional welding methods for polymers, including resistance welding, has significant issues, including additional weight deposition in joints, pre-welding preparations, the requirement for welding skill, welding consumables, and affluent, not to mention the problems associated with welding defects. Moreso, the arc welding processes traditionally employed in joining metal and alloys have not been able to join the polymers.

Friction stir welding (FSW) is a recent technology invented at 'The Welding Institute' in 1991. It has a great chance of solving most of the aforementioned problems [4]. At first, due to the limited technology of using non-consumable tools, industrial use of this process was limited to light alloys (typically aluminium alloys). Subsequently, FSW technology gave a good impression of withstanding highly adverse conditions of forces/torque at a high temperature, which are encountered when joining popular commercial materials like steels, stainless steels, and Ni/Ti alloys [5].

The FSW tool has a cylindrical shank with one of its ends called the shoulder. At the shoulder, a pin is made coaxially to the shank, and the pin is also called the probe. During the FSW, the tool is rotated, and the pin is fully inserted into the sheets, being joined until the shoulder makes contact with the upper surface of the sheet. The friction due to relative motion between the contacting work surface and the shoulder generates enough heat for the material to get softened and the rotation and simultaneous traverse of the tool causes the flow and transport of material, resulting in the joining of the two sheets. The joint properties significantly depend on the material flow, a function of the process temperature. The material flow will be accessible at higher temperatures and lower flow stress. The adequate temperature provides a better jointing process. The temperature evolution in the affected material and the heat-affected zone (HAZ) is essential to joint properties. Thermal modelling is significant in optimising the heat input's various FSW parameters.

The FSW equipment is expensive, mainly because the spindle and drive systems need a lot of power and torque. The FSW has been traditionally employed for metallic welding materials for two decades. Of late, due to several developments, FSW has come to compete powerfully with conventional welding processes and has extended to include machine learning applications [6], real-time monitoring [7], underwater welding [8], joining similar and dissimilar composite materials [9], and the ability to join polymers [10].

Compared with metals, the research on the investigation of FSW in polymers is very less, and it is still complicated due to the low thermal conductivity and wide variation in the rheological behaviours of the joint depending on the polymer molecule properties [11]. But, a surge in the use of polymers, even in the metal application, shifts the onus on the welding of polymers too. Whereas the joining technique of polymers is peculiarly different from metals and alloys, the efficiency of the joint made by FSW of polymers has been able to achieve 81% in the case of poly(methyl methacrylate) (PMMA) sheets [12]. Elyasi and Derazkola studied the thermomechanical and experimental effects of the FSW parameters and measured the temperature profile development of a PMMA T-joint. They indicated that the most elevated flexural (93% PMMA strength) and tensile (84% PMMA strength) strengths could be acquired [13]. Polymer joining techniques have been developed to include underwater FSW. The simulation results, supported by experimental results on polycarbonate (PC) polymers, showed that a lower heat concentration on the FSW joint line directly results from water's increased cooling capacity [14]. More than one study has tried to develop the conventional FSW of polymer–polymer or polymer-metal using innovative technologies such as friction stir additive manufacturing [15]. Technology development still needs to be improved despite the benefits, such as increased deposition rate and strong bonding [16].

Acrylonitrile butadiene styrene (ABS) is a lightweight material with a low glass transition temperature with a wide range of applications, including in the chemical and auto industries. ABS sheets are primarily used in the automotive industry because they can absorb energy from impacts and keep their shape. ABS is also a good choice for home appliances [17]. Typically, moulded ABS polymer products are employed in very large volumes in trains, buses, and trucks, to make door handles and liners, dashboards, seat belts, backs, pillar trim, etc. As ABS is an opaque thermoplastic, many studies have investigated the welding of similar and dissimilar thermoplastics joined by the FSW and FSSW methods [18]. They contain the FSW of ABS-PC [19,20], the joining of PMMA-ABS by the FSSW [21], and 3D-printed ABS materials [22].

Several studies tried understanding the behaviour of ABS plates during the FSW process. Mendes et al. [17] examined the welding parameters on the joining quality of the ABS sheets using a stationary shoulder without additional heat sources. The study indicated that the joint efficiency was 40% less than the efficiency at high tool rotational speed. Mendes et al. [23] developed a robotic system for joining ABS plates by FSW and examined the influential process factors. The study indicated that the robotic system gives a better joint performance compared to the robotic FSW and traditional FSW machines. Kumar and Roy [19] used a double-step shoulder to minimise excessive flash while joining polycarbonate (PC) and ABS sheets. The study examined the effects of welding velocity, rotational speed, tilt angle, and pin geometry. The results showed that the flash evolved from the PC to the ABS side. Kumar et al. [24] investigate the ability to join polyamide (PA6) to ABS to study dissimilar thermoplastic joining and overcome significant physical property variation. The investigation results demonstrated that adding specific ratios of aluminium powder as reinforcement to both plates can improve joining abilities via the FSW process. Hajideh et al. [25] reinforced the welding zone between the Polypropylene (PP) and ABS by incorporating copper powder and studied the mechanical properties as a function of process parameters: welding velocity, rotational speed, and preheating. The resultant joint strength reached 94% of that of polypropylene.

In order to optimise the weld quality, several tools, such as Taguchi methods, artificial neural networks (ANN), and the response surface method (RSM), have been employed [26]. Bagheri et al. [1,27]. RSM and analysis of variance (ANOVA) to optimise impact strength for ABS joints made by FSW. The results indicated that the impact strength significantly depends on the FSW parameters. Sadeghian et al. [28] investigated the effect of FSW parameters on the mechanical properties of ABS by employing RSM with a central composite design (CCD) coupled with ANOVA. The study found that the best conditions were when the speed was 900 rpm, the tilt angle was 2°, and the welding speed was 25 mm/min.

The future outlook of FSW for polymers has attracted huge interest from researchers and industry professionals. Keeping this in view, the present study considers a novel investigation of polymers joined by FSW using a pneumatically powered portable tool. The article studies the ability to replace the conventional FSW system (including an adapted vertical milling machine) with a pneumatically powered system for polymer repair applications, such as car bumpers, motorboats, and polymer vessels. The pneumatically powered tool was used to join the ABS sheets in butt joint configuration using FSW and friction stir spot welding (FSSW). The RSM and ANOVA were employed to optimise the process parameters for suitable heat input. The generated heat, tensile strength, microhardness, and micrographic analysis were examined in this study.

2. Materials and methods

The pneumatic-powered portable system was employed to power the FSW tool. The FSW tool was fixed inside the rotary driver. The Schneider SuperMaster 400-10-60 W compressor (Schnider, Germany) was used to develop and control the rotational speed and generate friction heat for polymer joining. In this experiment, the maximum rotational speed of 1400 rpm was used. The specifications of the compressor are shown in Table 1. Durable polyurethane hoses were used for connecting the compressor to the rotary screwdriver.

The conventional rotary drive was adapted through a novel design, with the holder replaced by a chuck to accept and hold the FSW tool. The FSW tool (made of HCHCr steel) has a shoulder with a diameter of 14 mm and a pin with a diameter of 3 mm and a length of 3.75 mm, while the opposite end of the tool has an 8 mm diameter neck that can be firmly fixed into the drives chuck (as shown in Figure 1). The overall length of the tool was 65 mm. The specifications of the FSW tool material are shown in Table 2.

Table 1. Air compressor specifications.

Suction power (l/min)	390
Inflation performance (l/min)	300
Drive power (kW)	2.2
Rotational speed (rpm)	1430
Discharge pressure (bar)	10

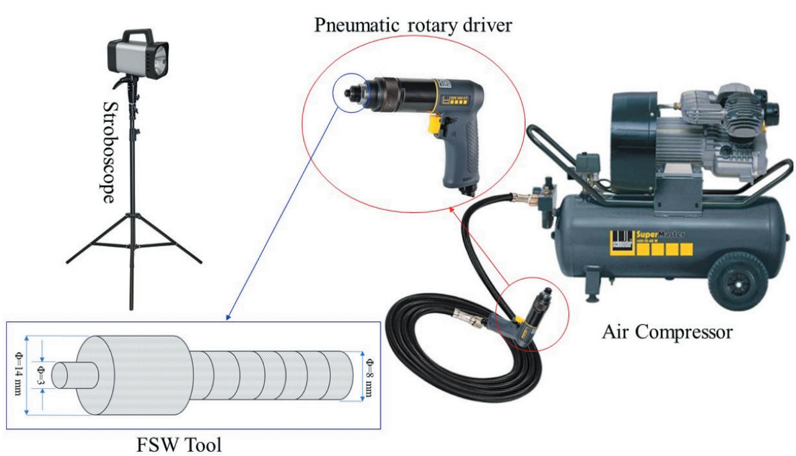

Figure 1. Pneumatic-powered portable friction stir welding components.

Table 2. Chemical composition (wt. %) of HCHCr tool material.

C	Si	Mn	P max	S max	Cr
1.9–2.2	0.1–0.6	0.2–0.6	0.03	0.03	11–13

The rotational speed of the tool was pneumatically controlled with the compressor system and could provide three different values of rotational speeds. A stroboscope was used to measure the rotating tool speed accurately. A stroboscope is an instrument for measuring the speed of rotating parts by shining a light that makes these parts appear to be moving slowly or stationary. Figure 1 shows the pneumatic friction stir welding components.

A manually controlled pneumatic rotary driver (PRD) was employed in this process. Important processes such as tool rotational speed and traversing velocity were selected and varied during FSW, and tool rotational speed and dwell time during the FSSW. Before carrying out the experiments, a trained technician was engaged of developing skills in operating the PRD and maintaining constant plunge position and traversing speed. This was important to keep and maintain the plunging force/plunge depth and tilt angle steady during the FSW/FSSW.

Acrylonitrile Butadiene Styrene (ABS) polymer sheets were 20 mm wide, 50 mm long, and 4 mm thick. The mechanical properties are shown in Table 3. The polymer sheets were prepared as butt joints, placed on an iron anvil and secured by wooden supports. The maximum temperature in the welding area was measured using an IR thermometer. The setup of the pneumatic-powered portable friction stir welding system is shown in Figure 2.

Table 3. Acrylonitrile butadiene styrene (ABS) properties [17].

Density (g/cm^3)	Tensile strength (MPa)	Strain break (%)	Glass transition temperature (°C)
1.04	40.5	50	105

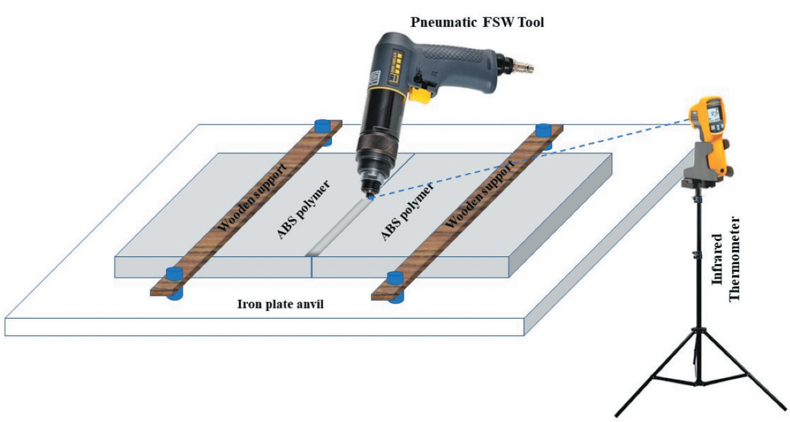

Figure 2. Pneumatic-powered portable friction stir welding setup.

Table 4. Maximum temperature for ABS welding zone during FSW and FSSW process.

	FSW			FSSW		
#	Rotational speed (rpm)	Traversing velocity (mm/s)	Temperature (°C)	Rotational speed (rpm)	Dwell time (sec)	Temperature (°C)
01	750	4	98	15	15	80
02	750	7	104	25	25	87
03	750	10	108	35	35	97
04	1000	4	101	15	15	91
05	1000	7	106	25	25	103
06	1000	10	105	35	35	108
07	1250	4	112	15	15	101
08	1250	7	110	25	25	109
09	1250	10	103	35	35	115

During the experiments, the FSW tool's rotation speed and traverse velocity were essential controlled process parameters, while for FSSW, the essential process parameters were rotational speed and dwell time. The tool rotational speed, traversing velocity (for FSW), and dwelling time (for FSSW) were varied in the ranges of 800–1300 rpm, 4–10 mm/s, and 15–30 s, respectively. Both friction stir welding (FSW) and friction stir spot welding (FSSW) were investigated to optimise the welding temperature. The welding zone temperatures were measured via an IR thermometer for real-time monitoring. The optioned maximum temperatures for the ABS welding zone for each experiment for both FSW and FSSW are shown in Table 4.

Several samples were cut out at and around the welding zone for mechanical performance analysis. The specimens were prepared according to the ASTM D638 [29] standard for the tensile test using an Instron 3400 universal tensile machine (Instron, USA) at room temperature. The specimens' microhardness was measured using RISH-TDV1000 (Ryf AG, France) according to ASTM E384–17 [30].

3. Response surface methodology (RSM)

When finding the optimal solution is a goal in industrial processes, response surface methodology (RSM) emerges as an easy and effective method. This method combines statistical and mathematical techniques to devise a solution that optimises the output based on several factors.

$$Y = \emptyset(x_1, x_2, \ldots .x_k) \pm e_r \tag{1}$$

$$Y = b_o + \sum b_i x_i + \sum b_{ij} x_i + \sum b_{ij} x_i x_j + e \tag{2}$$

Where the predicted output response is Y, b_o is a constant, and bi, b_{ii}, and b_{ij} are the linear, quadratic, and cross-product coefficients.

In most literature on response functions, the output variables are called response functions, while the input variables are referred to as independent variables. RSM has been used a lot in many areas of engineering, like mechanical, chemical, and manufacturing engineering. It has also grown to include new areas, like medical applications. Last year, the RSM method was computerised in several commercial software packages, such as MATLAB and Minitab. In this study, the RSM was used to optimise the welding temperatures.

4. Results and discussions

4.1. Temperature analysis

In this study, the maximum temperature response according to the variation of the process parameters was investigated. In RSM, the central composite design (CCD) was used based on Minitab 19 software. Two factors and three levels were used for both FSW and FSSW.

For FSW, the maximum temperature was examined according to the change in the rotation tool speed and welding velocity. Three levels of rotational speed were used: 750, 1000, and 1250 rpm, and three levels of welding velocity were also used: 4, 7, and 10 mm/min. Nine experiments were examined, as shown in Table 4. According to the result of ANOVA of FSW, as shown in Table 5, the rotational speed is the most influential factor on the welding temperature, where the F-Value is 20.35, which is much greater than the effects of welding velocity (F-Value is 2.26) in the linear model and square model. However, the interaction effect of (Rotational Speed*Welding Velocity) is greater than the effect of each substance.

Figure 3 indicates the variation of the temperature evolved during the pneumatic-powered FSW process with the variations in welding parameters. The temperature increases with an increase in the rotational speed. Within the selected range of rpm and welding velocity, the temperature is found to increase gradually with the increase in the welding velocity initially, followed by a gradual decrease. The highest temperature of 106°C was found to reach a welding speed of 7.5 mm/min.

As FSW is a solid-state process, the temperature of the weld does not exceed the melting point. The ABS polymer's melting point is about 200°C [31,32]. In all experiments in this study, the temperature did not reach more than 112°C, which indicates that no fusion or phase changes occurred. In the case of polymers, apart from melting, the glass transition temperature is another critical property and later tends to make the polymer structure viscous or rubbery [33]. The ABS glass temperature values are around 105°C [34,35]. So, for ABS sheets joined by the pneumatic-powered FSW, the user needs to use suitable conditions to keep them close to 105°C, so the resulting temperatures of around 104–106°C will be accepted. This temperature range can be achieved at rotational

Table 5. Analysis of variance for FSW for temperature vs rotational speed, welding velocity.

Source	DF	Adj SS	Adj MS	F-Value	P-Value
Model	5	148.028	29.606	16.07	0.022
Linear	2	41.667	20.833	11.31	0.040
Rotational Speed	1	37.500	37.500	20.35	0.020
Welding Velocity	1	4.167	4.167	2.26	0.230
Square	2	16.111	8.056	4.37	0.129
Rotational Speed*Rotational Speed	1	6.722	6.722	3.65	0.152
Welding Velocity*Welding Velocity	1	9.389	9.389	5.10	0.109
2-Way Interaction	1	90.250	90.250	48.98	0.006
Rotational Speed*Welding Velocity	1	90.250	90.250	48.98	0.006
Error	3	5.528	1.843		
Total	8	153.556			

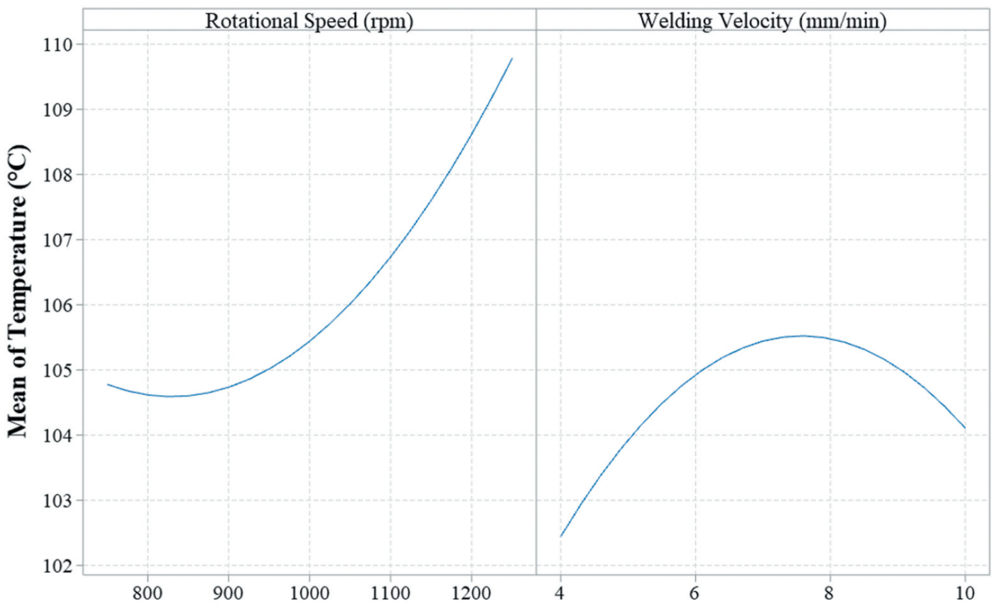

Figure 3. Variation of the FSW process temperature concerning the rotational speed (left) and welding velocity (right side).

speeds of 1050–1100 rpm with a wide range of welding velocities. For the interaction between the rotational speed and the welding velocity, the low rotational speed is less than 1050 rpm, and the welding velocity must be 6.5 mm/s, as shown in Figure 4a-b. At this parameter combination, a temperature of around 104–106°C was evolved, which is necessary for a good welding joint. The R-sq and R-sq(adj) values for the model were 96.40% and 90.40%, respectively. The predicted regression equation for the pneumatic-powered portable FSW is shown in Eq. (3).

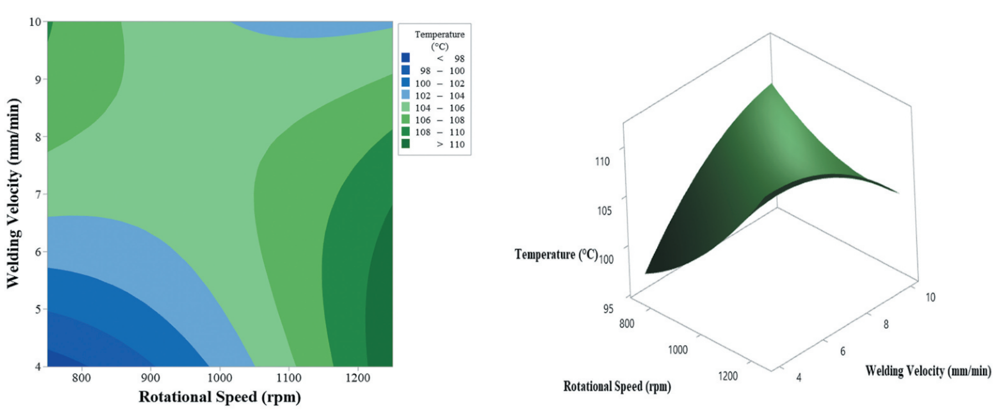

(a) (b)

Figure 4. Temperature distribution according to FSW parameters as a) contour plot and b) surface plot.

Table 6. Analysis of variance for FSW for temperature vs rotational speed, dwelling time.

Source	DF	Adj SS	Adj MS	F-Value	P-Value
Model	5	710.667	142.133	213.20	0.005
Linear	2	458.114	229.057	343.59	0.003
Rotational Speed (rpm)	1	439.744	439.744	659.62	0.002
Dwelling Time (s)	1	181.731	181.731	272.60	0.004
Square	2	2.409	1.205	1.81	0.356
Rotational Speed (rpm)*Rotational Speed (rpm)	1	1.556	1.556	2.33	0.266
Dwelling Time (s)*Dwelling Time (s)	1	0.389	0.389	0.58	0.525
2-Way Interaction	1	1.750	1.750	2.62	0.247
Rotational Speed (rpm)*Dwelling Time (s)	1	1.750	1.750	2.62	0.247
Error	2	1.333	0.667		
Total	7	712.000			

$$\text{Temperature} = 66.7 - 0.0043\text{N} + 9.98\text{V} + 0.000029\text{N}^2 - 0.241\text{V}^2 - 0.006333\text{N}^*\text{V} \quad (3)$$

In the case of pneumatic-powered FSSW, the rotational speed continues to remain the FSSW parameter, and the welding velocity (which was used as an FSW parameter) was replaced by dwelling time. The dwell time levels were selected as 15, 25, and 35 s. Also, as shown in Table 4, nine experiments were performed to find the optimum temperature. As shown in Table 6 (ANOVA), the rotational speed is the most influential factor on the welding temperature, where the F-Value is 659.62, which is about double the effect of dwelling time (F-Value is 272.60) in the linear model. The model can be considered a linear model where the values of the square and 2-way interactions are limited.

As shown in Figure 5, the temperature is proportional to rotational speed and dwell time. It is important to mention that, despite the long dwelling time, the temperature was kept within an acceptable range. The amount of air blown which passes through the tool

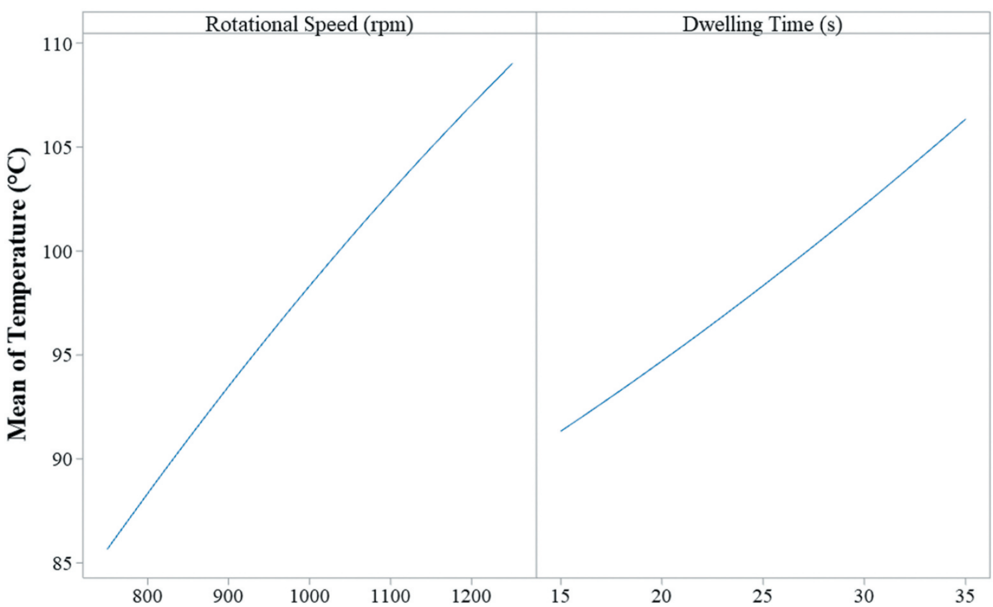

Figure 5. Variation of the FSSW process temperature concerning the rotational speed (left) and dwelling time(right).

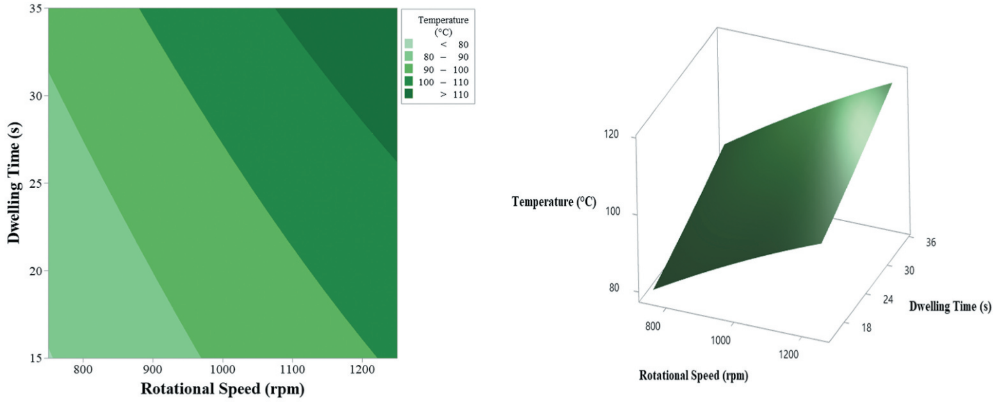

(a) (b)

Figure 6. Temperature distribution according to FSSW parameters as a) contour plot and b) surface plot.

was helping with surface cooling because it was focused on a single point. The behaviour was not found in the FSW process. As discussed in the FSW process, the values of the generated temperature must be kept around 104–106°C, which is necessary for a good welding joint. So, the suitable rotational speed is about 1000–1100 rpm and the dwelling time is around 15–25 s, as shown in Figure 6.

The resulting model was given an accepted model of R-sq 99.0%. The predicted regression equation for the pneumatic-powered portable FSW is shown in eq. 4.

$$\text{Temperature}(^{\circ}\text{C}) = 30.0 + 0.0687\text{N} + 0.100\text{t} - 0.000016\text{N2} + 0.00500\text{t2} + 0.000400\text{N}^{*}\text{t} \quad (4)$$

4.2. Mechanical performance

The pneumatic-powered portable friction stir welding tool was used for joining two sheets of ABS in butt joint configurations. Figure 7 shows that the left side represents the top and rear joint during pneumatic-powered FSW, while the right side represents the pneumatic-powered FSSW process; both the FSW and FSSW processes gave encouraging results.

Since the crack opening on the polymer surface usually occurs during the flexural test [36], which made the test less accurate, only the tensile and hardness tests were performed. The specimens were classified into three groups to understand the behaviour of the joints. The first group of FSW joints (9 specimens), the second group of FSSW joints (9 specimens) and two specimens represent the base metal. All 20 specimens were subjected to the tensile test using Instron 3400 universal tensile machine (Instron, USA) at room temperature according to the ASTM D638, as shown in Figure 8.

Figure 9 shows the behaviour of the maximum tensile load for each of the three groups. Most polymers cannot be subjected to the tensile test under high-capacity tensile testing. It is evident from the ABS polymer load–displacement curves (Figure 9a, b, and c) that the elongation of the base material revealed less ductilit. The FSSW specimens

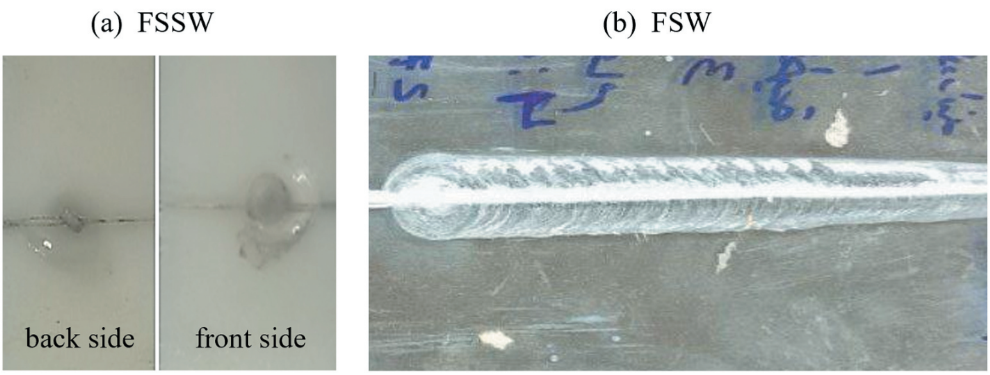

Figure 7. ABS welding joint appearance after pneumatic-powered (a) FSSW, (b) FSW.

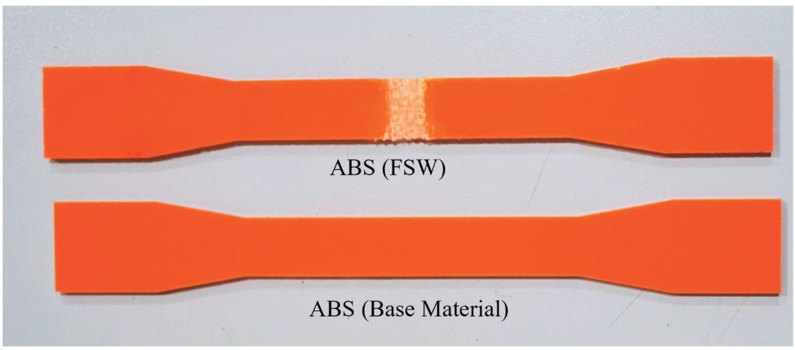

Figure 8. Tensile test specimens of ABS base material and FSW (ASTM D638).

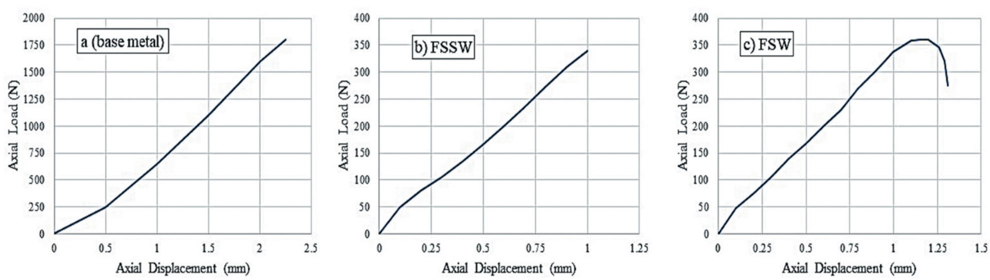

Figure 9. Flexural load–displacement curve for ABS sheets, a) base metal, b) FSSW, and c) FSW.

exhibited increased elongation, while the FSW specimens exhibited the highest ductility. The tensile test plots for FSW joints showed a linear relationship up to 350 N load at which 1 mm elongation was recorded (Figure 9c). Later, the ABS FSW specimens exhibited ductile behaviour until fracture. This novel and maiden portable welding gave a joint efficiency of approximately 20%. In any case, the efficiency of FSW joint of the order of 60% reported for ABS when fabricated on a proper professional machine [17,37]. However, the tensile behaviour of the polymer joints is comparable to several

Table 7. Average values of the microhardness.

Microhardness	Base Metal	Pneumatic-powered FSW	Pneumatic-powered FSSW
	15.3 HV	16.5 HV	18 HV

studies [17,24,38]. Such behaviour indicates that the welding zone shows ductile nature. The necking was found before the fracture.

Even though the load-bearing capacity of the manual pneumatic FSW is lower than the conventional FSW for ABS sheets, the results are encouraging, especially when developing the current tool to be an automated or semi-automated pneumatic FSW.

Furthermore, a large number of applications of polymers, such as in automobiles, home appliances and aircraft are non-load bearing and serve the requirements of aesthetic, used to cover and apron the interiors, internal mechanism. In such applications, this novel technique can become an out-of-box alternative in the repairs and fit-up. The portable nature of this welding system offers its ease for use in as-is-where-is condition in any orientation and 3D complex path which the conventional system is not capable of. As this is a novel and maiden preposition, its further development can improves its efficiency. The surface of joint produce is clear and has excellent finish make its application attractive.

It is possible to use hardness measurements to estimate the relative mechanical strength of welds in metallic and polymeric materials [23]. Besides the tensile test, the microhardness test was done using RISH-TDV1000 (Ryf AG, France) according to ASTM E384–17 to determine if the pneumatic source is quite enough to produce a good weld joint. In the FSW process of mechanical source, the welded zone's microhardness is relatively higher than the base metal. Forming operations can leave defects in the surfaces of materials, so in this study, hardness was measured in the welding heat-affected zone. The hardness was measured at several points on both sides of the weld line, and the average measurements were taken. As shown in Table 7, the welding hardness is unchanged concerning the hardness of the base material. Thus, hardness does not give helpful knowledge for the ABS sheets joined by FSW or FSSW.

5. Conclusion

In this article, the traditional FSW has been replaced by a portable, pneumatic-powered FSW to rotate the tool for ABS polymer joining and repairing. Besides being a portable facility, it can perform on-site welding on an as-is-where-is basis about any path in 3D space. It provides a better sustainable, clean, and cheap welding alternative.

Response surface method (RSM) and analysis of variance (ANOVA) were used to analyse the results.

The results for FSW and FSSW show that excellent weld quality was obtained when at tool rotational speed less than or equal to 1100 rpm. The welding speed of less than 6.5 mm/min (for FSW) and dwell time of 25 s or less (FSSW) were suitable for the good quality weld.

The evolved temperature of 105°C (in both processes) was suitable for good-quality welding.

The results of the tensile test and hardness test were encouraging. Even though the flexural load of the manual pneumatic FSW is still lower than the conventional FSW for ABS sheets, the results could be better, especially when developing the current tool to be an automated or semi-automated pneumatic FSW.

Disclosure statement

No potential conflict of interest was reported by the author(s).

ORCID

Raheem Al-Sabur http://orcid.org/0000-0003-1012-7681
M. Serier http://orcid.org/0000-0001-9145-5665
A. N. Siddiquee http://orcid.org/0000-0002-3573-8385

References

[1] Gareeva N, Starodubova A, Romanova A, "The evaluation of sustainable development for the manufacturers of construction-polymer products," in *E3S Web of Conferences* Kazan, Russia, 2021, vol. 274: EDP Sciences, p. 10007, 18(6):2021. doi:10.1051/e3sconf/202127410017.
[2] Oladele IO, Omotosho TF, Adediran AA. Polymer-based composites: an indispensable material for present and future applications. Int J Polym Sci. 2020;2020:1–12.
[3] Krause M. Technologies and innovations for the plastics industry: polymer 2030 Glauner, Patrick, Plugmann, Philipp. In: Innovative technologies for market leadership. London: Springer; 2020pp. 233–243 978-3030413088.
[4] Chikh A, Serier M, Al-Sabur R, et al. Thermal modeling of tool-work interface during friction stir welding process. Russian J Non-Ferrous Metals. 2022;63(6):690–700.
[5] Meran C, Canyurt O. Friction stir welding of austenitic stainless steels. parameters. 2010;6:13.
[6] Bahedh AS, Mishra A, Al-Sabur R, et al. Machine learning algorithms for prediction of penetration depth and geometrical analysis of weld in friction stir spot welding process. Metall Res & Technol. 2022;119(3):305.10.1051/metal/2022032
[7] Al-Sabur R, Jassim AK, Messele E, "Real-time monitoring applied to optimize friction stir spot welding joint for AA1230 Al-alloys," *Materials Today: Proceedings*, vol. 42, pp. 2018–2024, 2021, doi: 10.1016/j.matpr.2020.12.253.
[8] Khalaf HI, Al-Sabur R, Abdullah ME, et al. Effects of underwater friction stir welding heat generation on residual stress of aa6068-t6 aluminum alloy. Materials. 2022;15(6):2223.
[9] Bhardwaj N, Narayanan RG, Dixit U, et al. Recent developments in friction stir welding and resulting industrial practices. Adv Mater Process Technol. 2019;5(3):461–496.
[10] Al-Sabur R, Khalaf HI, Świerczyńska A, et al. Effects of noncontact shoulder tool velocities on friction stir joining of polyamide 6 (PA6). Materials. 2022;15(12):4214.
[11] Lambiase F, Derazkola HA, Simchi A. Friction stir welding and friction spot stir welding processes of polymers—State of the art. Materials. 2020;13(10):2291.
[12] Aghajani Derazkola H, Simchi A. Experimental and thermomechanical analysis of friction stir welding of poly (methyl methacrylate) sheets. Sci Tec Weld Joining. 2018;23(3):209–218.
[13] Elyasi M, Derazkola HA. Experimental and thermomechanical study on FSW of PMMA polymer T-joint. Int J Adv Manuf Technol. 2018;97(1):1445–1456.

[14] Derazkola HA, Garcia E, Elyasi M. Underwater friction stir welding of PC: experimental study and thermo-mechanical modelling. J Manuf Processes. 2021;65:161–173.
[15] Derazkola HA, Khodabakhshi F, Simchi A. Evaluation of a polymer-steel laminated sheet composite structure produced by friction stir additive manufacturing (FSAM) technology. Polymer Testing. 2020;90:106690. 10.1016/j.polymertesting.2020.106690
[16] Shen Z, Chen, S, Cui, L, et al. Local microstructure evolution and mechanical performance of friction stir additive manufactured 2195 Al-Li alloy. Mater Charact. 2022;186:111818.
[17] Mendes N, Loureiro A, Martins C, et al. Effect of friction stir welding parameters on morphology and strength of acrylonitrile butadiene styrene plate welds. Mater & Des. 2014;58:457–464.
[18] Iftikhar SH, Mourad A-HI, Sheikh-Ahmad J, et al. A comprehensive review on optimal welding conditions for friction stir welding of thermoplastic polymers and their composites. Polymers. 2021;13(8):1208.10.3390/polym13081208
[19] Kumar S, Roy BS. Novel study of joining of acrylonitrile butadiene styrene and polycarbonate plate by using friction stir welding with double-step shoulder. J Manuf Processes. 2019;45:322–330.
[20] Gao J, Shen Y, Xu H, "Investigations for the mechanical, macro-, and microstructural analyses of dissimilar submerged friction stir welding of acrylonitrile butadiene styrene and polycarbonate sheets," , vol. , no. , pp. , 2016 doi:10.1177/0954405415572663.
[21] Dashatan SH, Azdast T, Ahmadi SR, et al. Friction stir spot welding of dissimilar polymethyl methacrylate and acrylonitrile butadiene styrene sheets. Mater & Des. 2013;45:135–141.
[22] Kumar R, Singh R, Ahuja I, et al. Friction-stir-spot welding of 3D printed ABS and PA6 composites: flexural, thermal and morphological investigations. Adv Mater Process Technol. 2020;8(1):1–8.
[23] Mendes N, Loureiro A, Martins C, et al. Morphology and strength of acrylonitrile butadiene styrene welds performed by robotic friction stir welding. Mater & Des. 2014;64:81–90.
[24] Kumar R, Singh R, Ahuja I. Friction stir welding of ABS-15al sheets by introducing compatible semi-consumable shoulder-less pin of PA6-50al. Measurement. 2019;131:461–472.
[25] Hajideh MR, Farahani M, Ramezani NM. Reinforced dissimilar friction stir weld of polypropylene to acrylonitrile butadiene styrene with copper nanopowder. J Manuf Processes. 2018;32:445–454.
[26] Serier M, Gangil, Namrata, Chikh, Amina, et al., "Numerical study of a cantilever beam carrying a crack by response surface methodology," *Materials Today: Proceedings* November 12-13, 2022 New Delhi, India, 2022 doi:10.1016/j.matpr.2022.01.438.
[27] Bagheri A, Azdast T, Doniavi A. An experimental study on mechanical properties of friction stir welded ABS sheets. Mater & Des. 2013;43:402–409.
[28] Sadeghian N, Givi MKB. Experimental optimization of the mechanical properties of friction stir welded acrylonitrile butadiene styrene sheets. Mater & Des. 2015;67:145–153.
[29] Xiao X. Dynamic tensile testing of plastic materials. Polymer Testing. 2008;27(2):164–178.
[30] A. S. f. Testing and Materials. ASTM E384: standard test method for microindentation hardness of materials. PA 19428-2959. United States: ASTM West Conshohocken; 2017.
[31] Li Y, Shimizu H. Improvement in toughness of poly (l-lactide)(plla) through reactive blending with acrylonitrile–butadiene–styrene copolymer (ABS): morphology and properties. Eur Polym J. 2009;45(3):738–746.
[32] Smith P, Weder C. Conducting polymers, solution-and gel-processing of. Encycl of Mater: Sci and Technol. 2011;1497–1504.
[33] Hedvat S. Molecular interpretation of T//, the rubbery-viscous 'transition'temperature of amorphous polymers. Polymer. 1981;22(6):774–777.
[34] Wilkes CE, Summers JW, Daniels CA, et al. PVC handbook. Munich: Hanser; 2005 3446227148.

[35] Rahman M, Schott N, Sadhu LK, “Glass transition of ABS in 3D printing,” in *COMSOL Conference*, *Boston, MA*, 2016.

[36] Eyvazian A, Hamouda AM, Aghajani Derazkola H, et al., “Study on the effects of tool tile angle, offset and plunge depth on friction stir welding of poly (methyl methacrylate) T-joint,” *Proceedings of the Institution of Mechanical Engineers, Part B: Journal of Engineering Manufacture*, vol. 234, no. 4, pp. 773–787, 2020.

[37] Pirizadeh M, Azdast T, Ahmadi SR, et al. Friction stir welding of thermoplastics using a newly designed tool. *Mater & Des (1980-2015)*. 2014;54:342–347.

[38] Kyratsis P, Tzetzis D, “Investigation of the mechanical properties of acrylonitrile butadiene styrene (ABS)-nanosilica reinforced nanocomposites for fused filament fabrication 3D printing,” in *IOP Conference Series: Materials Science and Engineering* 28-31 Mar 2018 Timisoara, Romania, 2018, vol. 416, no. 1: IOP Publishing, p. 012086.